
Article:
Jegede, OE, Haque, N, Mullis, AM et al. (2021) Solidification transformations in liquid phase separated metastable monotectic Cu – 50 at.% Co alloy. Canadian Journal of Chemistry. ISSN: 0008-4042

https://doi.org/10.1139/cjc-2021-0064

Solidification transformations in liquid phase separated metastable monotectic Cu – 50 at. % Co alloy.

Oluwatoyin E. Jegede [a*], Nafisul Haque [a,b,] , Andrew M. Mullis [a] and Robert F. Cochrane [a]

[a] School of Chemical & Process Engineering, University of Leeds, Leeds LS2 9JT, UK.

[b] Department of Metallurgical Engineering, NEDUET, University Road, Karachi 75270, Pakistan

*Corresponding author: Oluwatoyin E. Jegede (email: pmoej@leeds.ac.uk)

Metastable monotectic Cu – 50 at. % Co alloy produced by arc melting has been processed under micro gravity condition using a drop tube and subjected to differential thermal analysis (DTA). Microstructural evidence from the as solidified sample revealed that rapid cooling of the arc melt process was enough to incite liquid phase separation in the alloy. In the drop tube samples, the melting temperature of the β- phase (Cu – rich) was determined to be 1294.8 K while that of the α- phase (Co – rich) was found to vary with cobalt content.

Keywords: Liquid phase separation, Monotectic solidification, Differential thermal analysis (DTA), Drop tube, metastable alloys.

1 INTRODUCTION

There has been significant research on the equi – atomic Cu – Co alloy ($Cu_{50}Co_{50}$) due to the symmetrical metastable miscibility gap (MG) said to exist in the alloy system [1–3]. Nakagawa [1], Robinson et al. [2] and Elder et al. [3] all observed a metastable MG whose highest point (critical point) corresponds to the equi – atomic composition. Different values have been cited for the critical undercooling necessary to bring about liquid phase separation (LPS) in the alloy; the value was placed at 96 K below its equilibrium liquidus by Yamauchi et al. [4], 90 K was reported by Nakagawa [1] while Robinson et al. [2] reported 80 K. The peritectic reaction of the system has been said to occur at the temperature (Tp) of 1385 K. However, the accepted MG of the system is that determined by Cao et al. [5] using DTA and glass fluxing on alloys of composition 16 – 87.2 at. % Co. This slightly symmetrical MG had critical composition of 53 at. % Cu and a binodal boundary with composition range of 16 – 89.3 at. % Cu. Liquid phase separation was found to occur at this critical composition at temperature of 1547 K which was 108 K below its equilibrium liquidus. Palumbo et al. [6] however stated that the critical point of the MG occurred at 58.5 at. % Cu with a temperature of 1556 K.

Generally, LPS occurs in the Cu – Co alloy system into L_1 (Co – rich) and L_2 (Cu – rich) phases when the parent melt is undercooled into the MG beyond a certain temperature limit (Tsep) which is composition dependant [4,7,8]. The solidification path of the demixed liquids differ to each other and to the initial homogeneous melt when traced on the metastable phase diagram due to each liquid having different undercooling. Also, secondary liquid phase separation of one liquid phase inside another has been said to occur at high undercooling due to truncated diffusion [7].

Different microstructures have been reported in this alloy [2,4,7–11]. Liquid phase separated structures have been reported at varying degree of undercooling. Yamauchi et al. [4] observed liquid phase separated features at undercooling of 123 K while in the long drop tube experiment (105 m), LPS was said to occur at undercooling of 300 K a value which exceeds the metastable phase diagram estimate for an alloy of such bulk composition [8]. In electro magnetic levitation (EML) studies carried out by Zhang et al. [10] and Davidoff et al. [11]on the alloy, liquid phase separated features were also reported. Davidoff et al. [11] using a combination of EML and splat quenching, observed that in splat quenched samples at estimated cooling rates of 10^7 Ks^{-1} an undercooling of 220 K is achieved and the microstructural morphology consisted of large coagulated Co – rich phase that showed evidence of secondary liquid phase separation a conclusion based on the presence of dispersed L_2 – rich particles in it. At higher cooling rates (magnitude of 10^6 to 10^7 Ks^{-1}); spinodal decomposition was observed [11]. In their EML sample on the other hand, the microstructural morphology at undercooling above 120 K consisted of large distorted / spherical particles with very high copper content (96 at. % Cu) in a L_1 - rich matrix (84 at. % Co). The interface between the two liquids had dendrites extending from the L_1 – rich phase into the L_2 – rich phase an indication they were likely formed post solidification of the Co – rich phase [11]. However, in the EML study of Munitz and Abbaschian [7] they undercooled the alloy to above 110 K and did not observe any evidence of LPS but rather zones of fine and coarse dendrites whose distinctive boundaries were observed to fade with increasing undercooling. They also observed that at 200 K, the elements of the coarse dendrites were found within the fine dendritic zones. The existence of distorted spherulites in other compositions was cited as evidence of LPS in those alloys. This is a probability as the distorted nature of the spherulites is thought to be as a result of the convective flow induced by the electromagnetic

stirring during the EML process. This is however not expected to be observed in drop tube experiments one of which reported the presence of core shell microstructures in the alloy [12]. The core shell microstructures resulted from the interplay of interfacial energies and temperature and or composition gradient leading to Marangoni motion of dispersed particles of the minority phase formed close to the surface of the parent droplets to the center of the parent droplet where they converge to form a core. Mechanism of formation and characteristics of these microstructures in drop tube processed 50 at. % Co alloy is available in literature [12,13]. Other researchers have also reported that the alloy is dendritic and that LPS is only feasible in the alloy at higher degree of undercooling [2,8,9]. Even though the alloy has been extensively researched there has been little report of phase separation in the alloy which is contrary to the calculations of the metastable phase diagram reported in [12] which states that the alloy should be able to phase separate both spinodally and by binodal phase separation after the critical alloy because of the minimal undercooling estimated to get the alloy into the miscibility gap. Undercooling is difficult to determine in drop tube experiments however, it can be inferred from the cooling rate which can be estimated from the diameter of droplets obtained in drop tube experiments using balance of heat fluxes within the falling droplet as described in [14].

In this article, differential thermal analysis (DTA) is used to gain insights into the accuracy of the calculated metastable phase diagram of the Co – Cu alloy system described in [12] as well as to understand the solidification transformations in drop tube processed Cu – 50 at. % Co alloy.

2 EXPERIMENTAL METHODS

The Cu – 50 at. % Co alloy was produced by alloying pure Co (99.998 %) and Cu (99.999 %) in an arc melting furnace with a protective argon atmosphere. The arc melting process was repeated nine times to ensure homogeneity of the ingot. Slices from the arc melt ingot were then processed in a 6.5 m drop tube under a nitrogen environment. The drop tube was evacuated to 10^{-4} Pa and back filled with nitrogen gas to 40 kPa. The alloy sample inductively heated was super-heated to 200 K above its equilibrium liquidus and injected into the drop tube and a dispersion of droplets of varying size solidified during their free fall down the tube. The collected droplets were sieved into standard sieve size fractions. Due to the limited amount of sample retrieved from the drop tube, samples from the sieve size fraction with the most amount of powder available were selected for DTA measurements (i.e. 850^{+} and < 38 μm). 31.4 mg and 9.7 mg of powder from the 850^{+} and < 38 μm size fractions respectively were measured out and melted in Al_2O_3 crucibles using a PerkinElmer™ STA 8000 simultaneous thermal analyser at heating and cooling rates of 15 $Kmin^{-1}$. Only the first heating and cooling cycle curves were considered in this study as the samples showed signs of Cu oxide contamination (samples had black appearance) and this is thought to be the origin of some of the peaks observed in the second process cycle. Also, that DTA curves from the second process cycle upwards are not likely to be representative of the starting alloy composition. Baseline artefacts identified on the curves were not discussed as they are not part of the transformation details of the alloy but of the reference sample hence they were subtracted from all DTA curves.

All the samples were then metallographic processed and their microstructure examined with a BX51 Olympus optical microscope fitted with a Zeiss AxioCam™ MRc5 camera and a Carl Zeiss Evo MA 15 SEM fitted with energy dispersive X-ray spectrometer (EDS). Backscattered electron imaging (BSE) mode was employed.

3 RESULTS AND DISCUSSION

The metastable phase diagram in [12] (figure 1) had critical composition of 58.7 at. % Cu and liquidus temperature of 1636 K. The estimated undercooling for LPS to occur in this critical alloy either by nucleation in the binode region or spinodally within the spinode was placed at 13 K. The Cu – 50 at. % Co alloy was estimated to undergo binodal LPS at undercooling of 41 K and spinodal decomposition at 52 K. The liquidus temperature of the alloy was determined to be 1639 K.

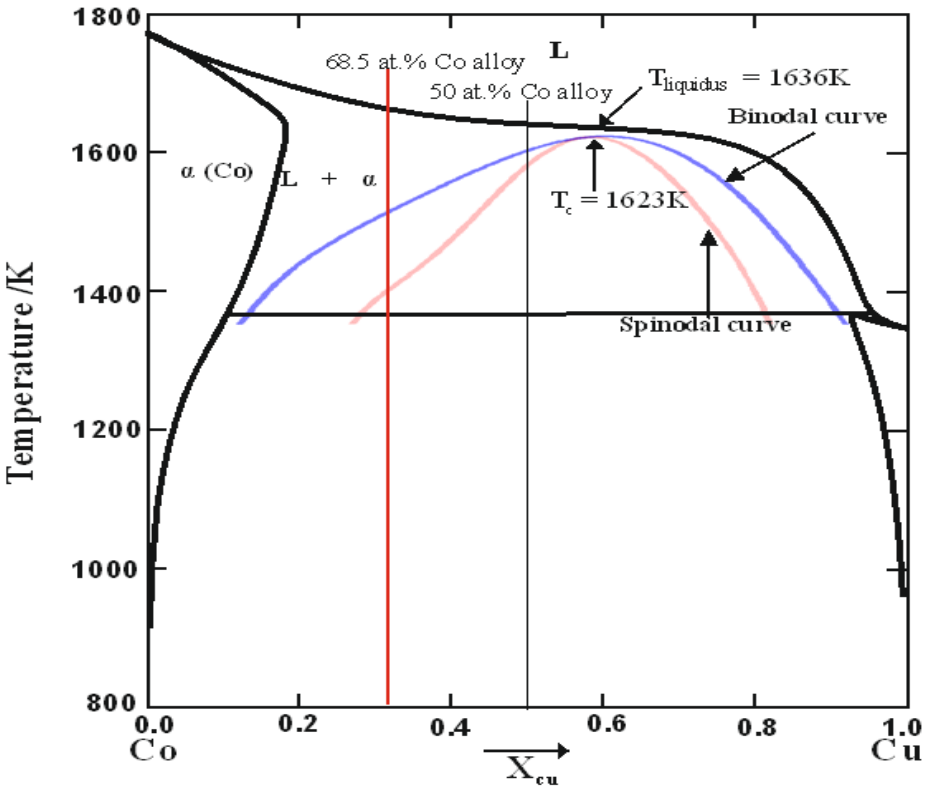

Figure 1: Metastable phase diagram of the Cu – Co system with super imposed miscibility gap [12]. Black vertical line shows the solidification path of the Cu – 50 at. % Co alloy.

Slices from the arc melt ingot showed two regions, one having a homogeneous appearance and the other which appeared unmixed contained a huge region of un-melted cobalt surrounded by

Co – rich coarse dendrites which decreased in size away from it towards the bottom of the sample. In the homogeneous section, shown by the optical micrograph in figure 2, dark structures dispersed in a light matrix in regions close to the copper hearth of the arc melt furnace are observed (figure 2a). These particles appear clustered in some areas. The appearance of the un-clustered particles looked like columnar structures and these were initially thought to be dendrites similar to the zones of fine and coarse dendrites observed by Munitz and Abbaschian [7] in the alloy but these were revealed to be spherical and spheroidised at higher magnification (figure 2b). EDS analysis (figure 3) gave the average composition of the dark particles as 87.6 at. % Co while the light matrix was observed to be Cu – rich. The microstructure also revealed considerate particle free zones indicating the volume fraction of the dispersed Co – rich particles in the matrix was low. These images seem to suggest the arc melted Cu – 50 at. % Co alloy had undergone LPS.

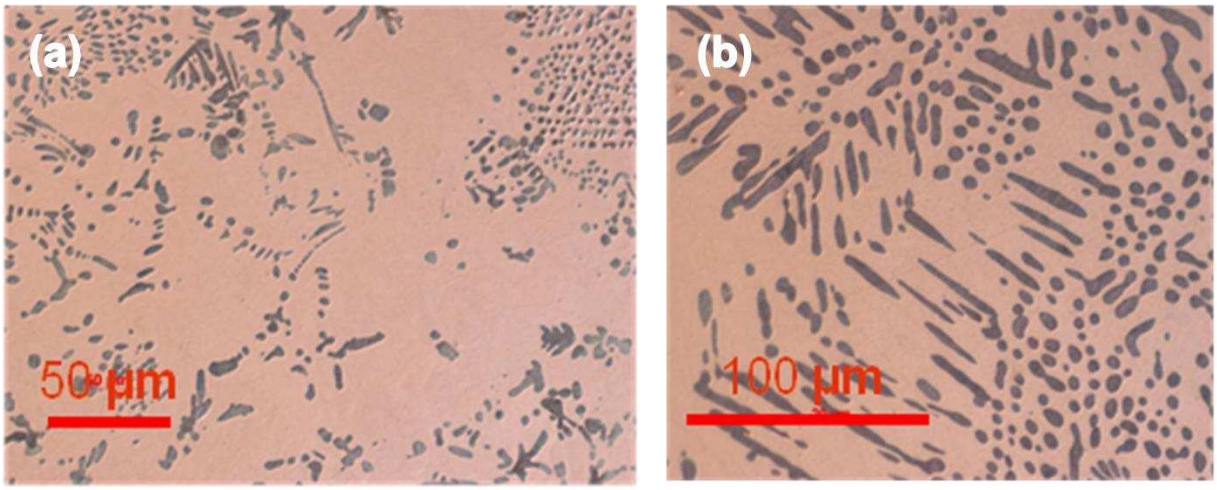

Figure 2: Optical microscopy images of slices of arc melt ingot of Cu – 50 at. % Co alloy, (a) shows dark cobalt rich structures in a copper rich matrix, (b) magnified view of the dispersed spherical particles.

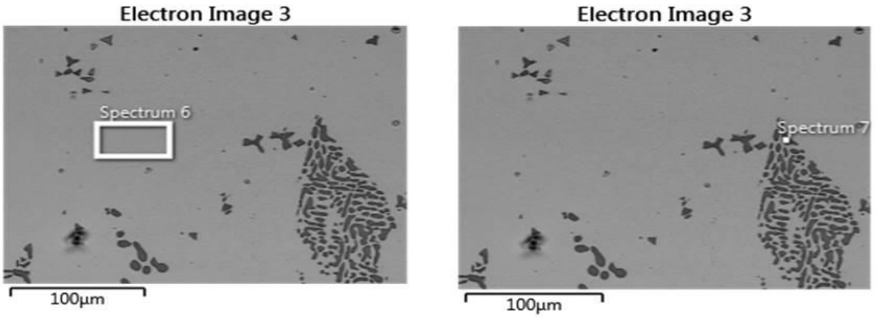

Element	At. %	
	Spectrum 6	Spectrum 7
Co	4.59	70.28
Cu	95.41	29.72

Figure 3: EDS readings of the matrix and of the dark inclusions respectively.

Extensive classification of structures observed in undercooled drop tube processed Cu- Co alloys have been given in literature [12]. These structures are basically of two categories; liquid phase separated structures and non – liquid phase separated structures. Figure 4a – d shows some of the reported microstructures.

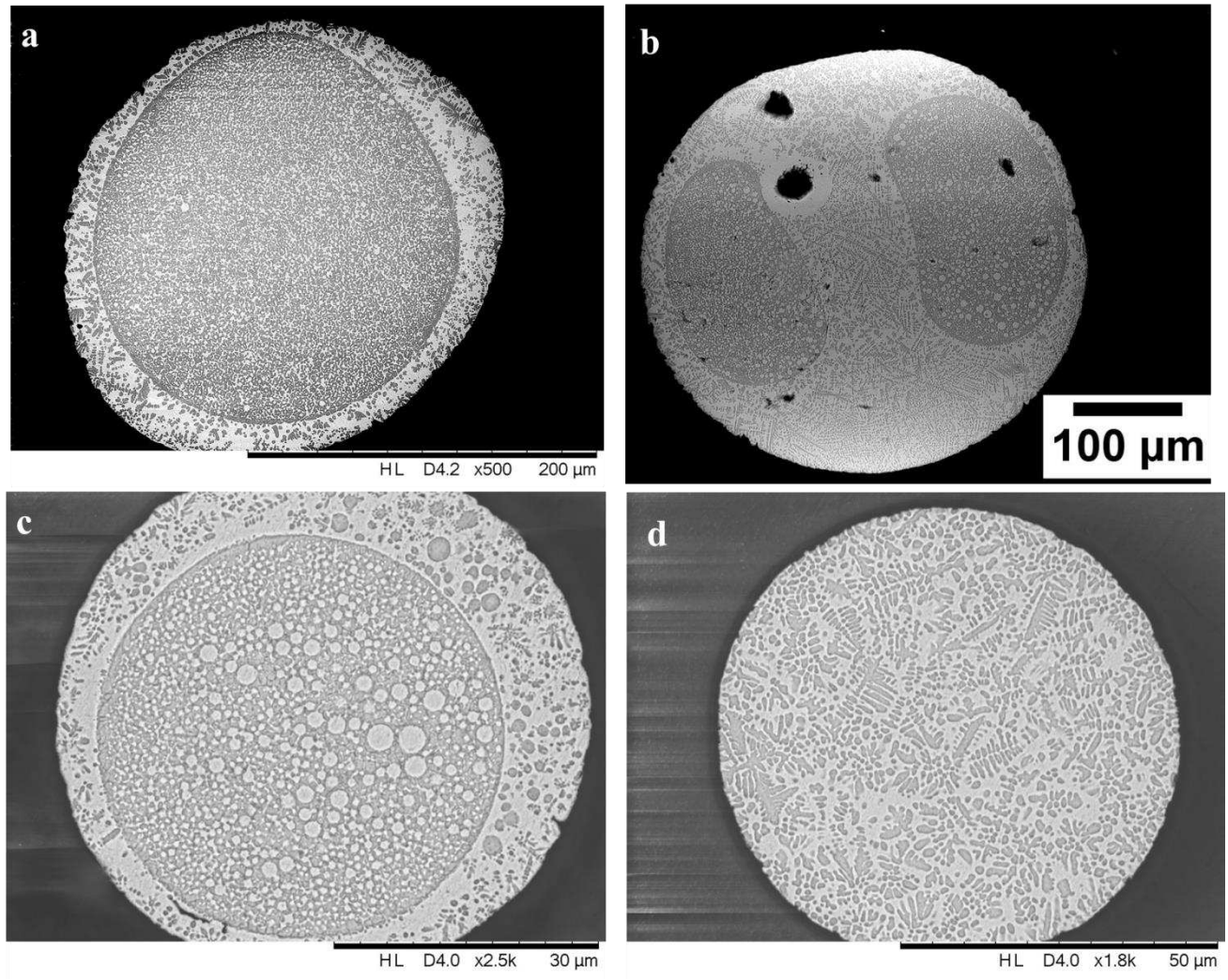

Figure 4: Back scattered SEM images of reported microstructures in undercooled drop-tube processed Co-Cu alloys, dark phase is Co – rich while the lighter phase is Cu – rich. (a) and (b) are evolving core shell structures of diameters 250 µm and 410 µm respectively, (c) 60 µm fully evolved core shell structure and (d) 72 µm dendritic structure [12].

The microstructure of the arc melt sample of the alloy presented in figure 2 establishes the occurrence of LPS in the alloy. This is evidenced by the dispersion of minority Co – rich spherical particles in a majority Cu – rich matrix. The appearance of these nucleated spherical particles indicates the alloy was successfully undercooled into the binodal region of the MG since nucleation is not known to occur under the spinodal curve. The migration and growth of

these particles in the binodal region occurs by diffusion and this could explain the clustering nature of the spherical particles which could be an indication of high rate of transport and this in turn is expected to lead to coarsening effect but the particles appeared to be of uniform size. No microstructural evidence was found to suggest concentration gradient in any of the arc melt slices; it is therefore likely the migration of these particles was due to temperature variation. At close proximity to the copper hearth, thermal gradient is higher and as such Marangoni convection move the particles away from the cooler end however, this may have been overwhelmed by flow induced by the arc's electric current which would also explain the spheroidised / rod – like appearance of some of the Co – rich particles. At the extreme end away from the copper hearth, the temperature difference is not as high but due to minute density difference between cobalt and copper, Stokes effect which should be prominent is rather negligible. This would explain why most of the particles are clustered at this side of the particle.

The arc melt sample was not used for DTA due to its majorly inhomogeneous appearance and apparent difficulty in extracting the homogeneous section. However, in the 850+ drop tube powder the first cycle heating curve (figure 5) had two endothermic peaks at 1385.5 K and 1645.6 K with onset temperatures of 1294.8 K and 1522 K respectively. Due to the fact that the microstructure in figure 6a revealed no evidence of metastable phase transformation these temperatures are analyzed using the equilibrium phase diagram. The first onset (1294.8 K) falls within $\alpha + \beta$ region with the α – phase (i.e. Co – rich) having volume fraction of 50.7 at. %. Since the alloy has equal atomic volume at this temperature, the observed peak is assumed to be due to release of heat of fusion on melting of the β – phase which is Cu – rich. Hence melting temperature (T_m) of the Cu – rich β – phase is taken as 1294.8 K (melting point of pure copper is

1358 K). The second endothermic onset falls within L + α region. There is however, more α – phase in this region than the liquid phase with α – phase having a volume fraction of 53 %. The α - Co rich phase contained 83.8 at. % Co while the composition of the liquid phase is shown to contain 12.5 at. % Co. The melting temperature of α – phase is taken as 1522 K (melting point of pure cobalt is 1768 K).

On the cooling curve two prominent exothermic events can also be observed. The first event had an onset temperature of 1589 K which is a shift of 67 K to its corresponding endothermic event. This temperature is also traced to the L + α region on the equilibrium phase diagram however, the composition of the liquid had increased to 19.4 at. % Co. The compositional increase is thought to be the reason for the shift between the endothermic and exothermic peaks as during solidification the composition is constantly being adjusted. The volume fraction of α – Co phase was determined to be 48.9 %. The nucleation temperature (T_N) of α – Co phase is therefore taken as 1589 K. The second exothermic onset corresponded to the solidification temperature (T_s) of the Cu – rich phase.

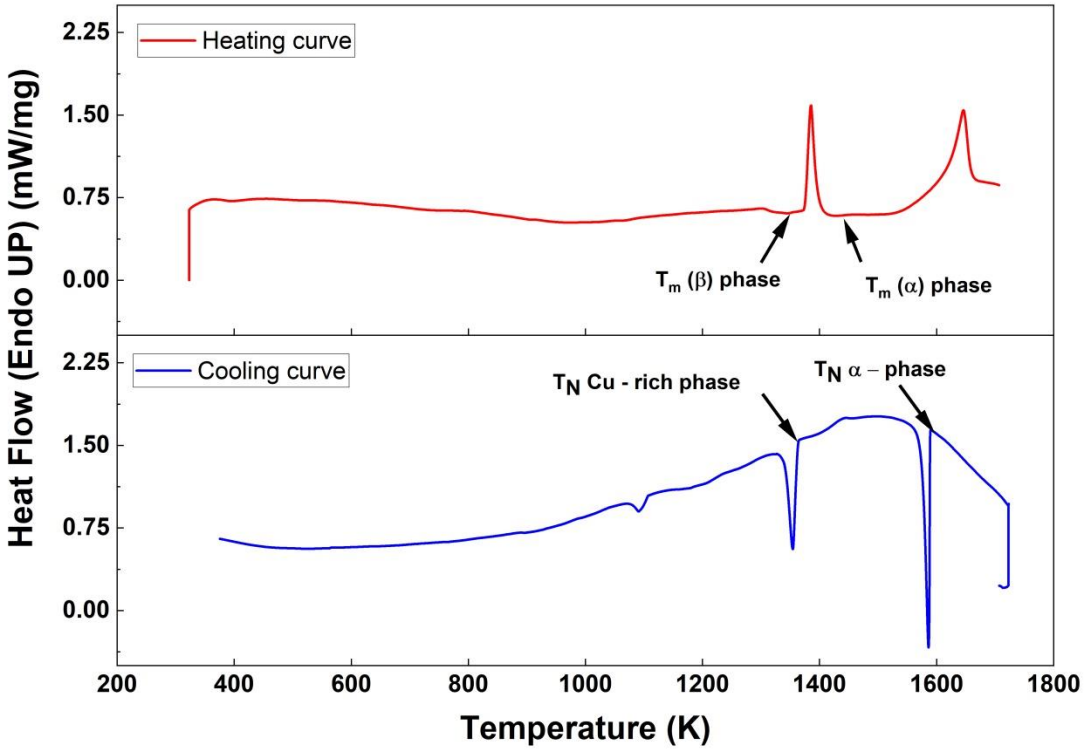

Figure 5: DTA plots of the 850+ µm drop tube powder of the Cu – 50 at. % Co alloy.

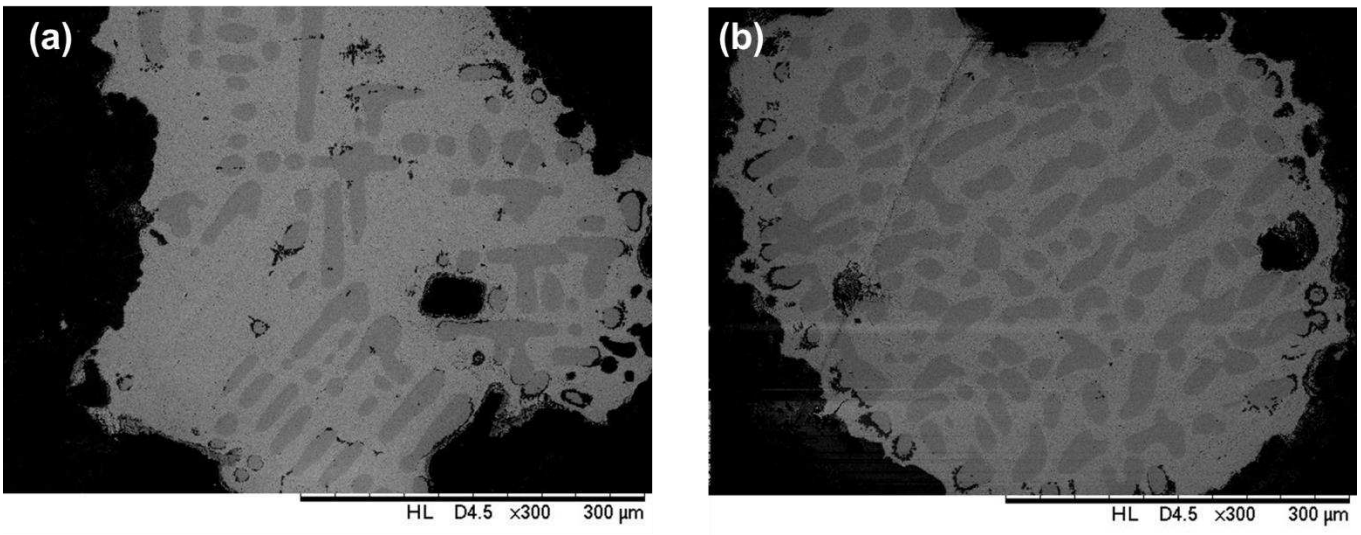

Figure 6: SEM images of DTA processed drop tube powder of the Cu – 50 at. % Co alloy: (a) 850+ µm powder size, (b) < 38 µm powder size.

In the < 38 μm drop tube powder size, two endothermic events were also observed on its heating curve (figure 7). The microstructure of the sample shown in figure 6b also displayed no signs of metastable transformation hence the equilibrium phase diagram is also used in analysing its DTA plot. The first onset temperature (1374 K) corresponds to the T_m of the Cu – rich phase having a composition of 94.3 at. % Cu. A second endothermic event signified by a broad peak had an onset temperature of 1621 K which is also traced to the L + α region however, the liquid composition (71.6 at. % Cu) is lesser than that of the 850+ μm powder. Volume fraction of α – Co phase is calculated to be 40.6 %. On the cooling curve, alloy at the onset temperature of the first exothermic peak (1613 K) has composition of 74.8 at. % Cu which is observed lower than that in the larger powder size. This is thought to be the temperature at which α – Co starts to nucleate (T_N). Volume fraction of the Co – rich phase had however reduced to 49.9 %. Onset temperature of the second exothermic peak (1383 K) which corresponds to the T_s of the Cu – rich phase is higher than that observed for the 850+ powder size. The volume fraction of α – Co phase was also observed to have increased to 53 %.

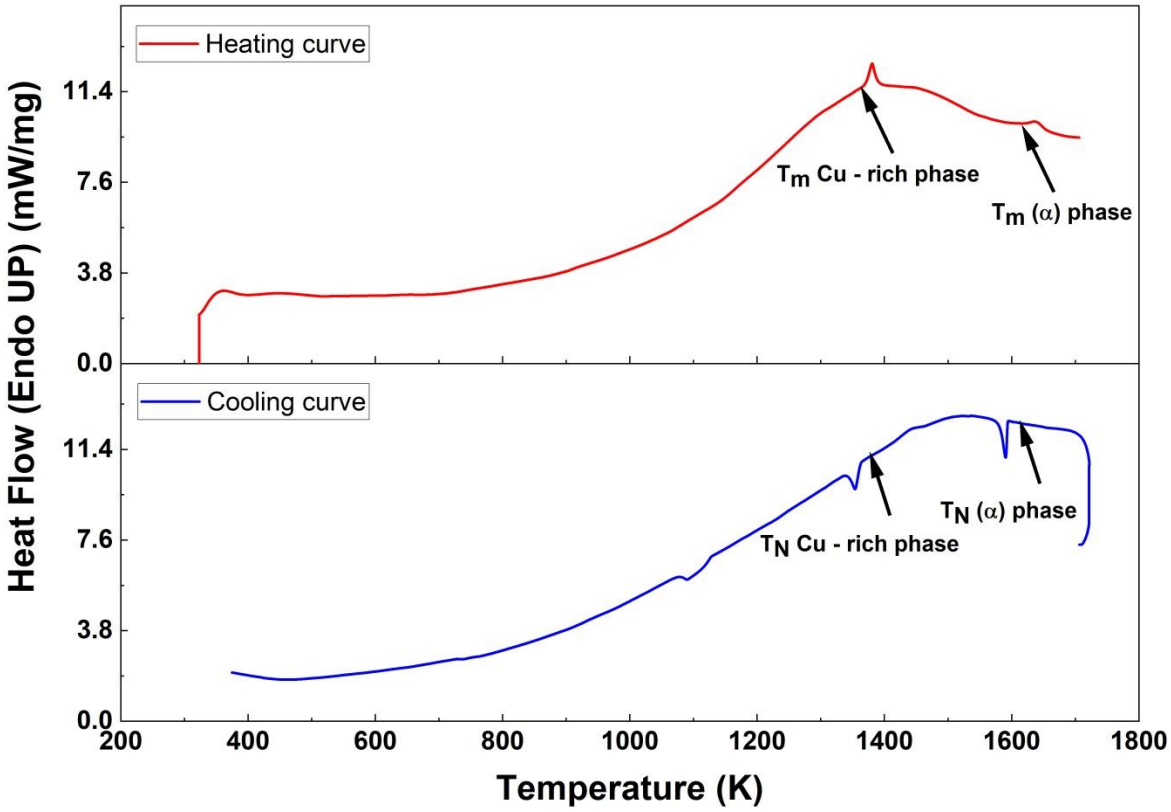

Figure 7: DTA plots of the < 38 µm drop tube powder of the Cu – 50 at. % Co alloy.

The value quoted for the liquidus temperature in the phase diagram in figure 1 is lower than that quoted by Davidoff et al. [11] who quoted 1655 K as the liquidus of the alloy and an estimated undercooling of 106 K to get into the binode. However, their values seem not supported by their phase diagram. According to their calculations, the critical composition of their MG was 52.7 at. % Cu with corresponding temperature of 1547 K, they also stated that their miscibility gap was symmetrical. If that is the case, the Cu – 50 at. % Co alloy is very close to their critical composition and as such expected to contact the binode curve very close to the temperature of their critical alloy.

4 CONCLUSION

The occurrence of LPS in the arc melt sample is contrary to previous cited works which concludes that the alloy is dendritic unless when subjected to high undercooling into the MG. Although the temperature and cooling rate of the arc melt processing is unknown, the fact that rapid cooling of the process was able to cause LPS to occur in the alloy is an indication that the undercooling required to cool into the MG is not as large as indicated in those literature but in line with the predictions of the calculated metastable phase diagram in figure 1.

Dendritic structures consistent with equilibrium phase diagram predictions were observed in the DTA samples of the drop tube processed powders. The melting temperature of the Cu – rich and Co – rich liquids was found to vary with droplet size which is also in line with phase diagram prediction. There is increased undercooling in smaller droplets which in turn favours the enrichment with the Co – rich phase. The higher the cobalt content, the higher the melting point of the two phases.

ACKNOWLEDGEMENT

Oluwatoyin Jegede is a commonwealth scholar, sponsored by the UK government.

COMPETING INTEREST STATEMENT

The authors declare there are no competing interests.

AUTHOR CONTRIBUTION STATEMENT

All authors actively contributed towards the writing of the manuscript and have given approval to its final version.

REFERENCES

[1] Y. Nakagawa, Liquid immiscibility in copper-iron and copper-cobalt systems in the supercooled state, Acta Metall. 6 (1958) 704–711. https://doi.org/10.1016/0001-6160(58)90061-0.

[2] M.B. Robinson, D. Li, T.J. Rathz, G. Williams, Undercooling, liquid separation and solidification of Cu-Co alloys, J. Mater. Sci. 34 (1999) 3747–3753. https://doi.org/10.1023/A:1004688313591.

[3] G. Elder, SP and Munitz, A and Abbaschian, Metastable Liquid Immiscibility in Fe-Cu and Co-Cu Alloys, Mater. Sci. Forum. 50 (1989) 137–150.

[4] I. Yamauchi, N. and Ueno, M. and Shimaoka, I. and Ohnaka, Undercooling in Co – Cu alloys and its effect on solidification structure, J. Mater. Sci. 33 (1998) 371–378. https://doi.org/10.1023/A:1004319829612.

[5] C.. Cao, G.. Görler, D.. Herlach, B. Wei, Liquid–liquid phase separation in undercooled Co–Cu alloys, Mater. Sci. Eng. A. 325 (2002) 503–510. https://doi.org/10.1016/S0921-5093(01)01756-7.

[6] M. Palumbo, S. Curiotto, L. Battezzati, Thermodynamic analysis of the stable and metastable Co–Cu and Co–Cu–Fe phase diagrams, Calphad. 30 (2006) 171–178.

https://doi.org/10.1016/J.CALPHAD.2005.10.007.

[7] A. Munitz, R. Abbaschian, Microstructure of Cu-Co Alloys Solidified at Various Supercoolings, Metall. Mater. Trans. A. 27 (1996) 4049–4059. https://doi.org/10.1007/BF02595654.

[8] A. Munitz, R. Abbaschian, Two-melt separation in supercooled Cu-Co alloys solidifying in a drop-tube, J. Mater. Sci. 26 (1991) 6458–6466. https://doi.org/10.1007/BF00551897.

[9] A. Munitz, R. Abbaschian, Liquid separation in Cu – Co and Cu – Co – Fe alloys solidified at high cooling rates, Mater. Sci. 33 (1998) 3639–3649.

[10] Y.K. Zhang, J. Gao, D. Nagamatsu, T. Fukuda, H. Yasuda, M. Kolbe, J.C. He, Reduced droplet coarsening in electromagnetically levitated and phase-separated Cu-Co alloys by imposition of a static magnetic field, Scr. Mater. 59 (2008) 1002–1005. https://doi.org/10.1016/j.scriptamat.2008.07.005.

[11] E. Davidoff, P.. Galenko, D.. Herlach, M. Kolbe, N. Wanderka, Spinodally decomposed patterns in rapidly quenched Co–Cu melts, Acta Mater. 61 (2013) 1078–1092. https://doi.org/10.1016/J.ACTAMAT.2012.10.010.

[12] O.E. Jegede, R.F. Cochrane, A.M. Mullis, Metastable monotectic phase separation in Co–Cu alloys, J. Mater. Sci. 53 (2018) 11749–11764. https://doi.org/10.1007/s10853-018-2417-y.

[13] A.M. Mullis, O.E. Jegede, T.D. Bigg, R.F. Cochrane, Dynamics of core--shell particle formation in drop-tube processed metastable monotectic alloys, Acta Mater. 188 (2020) 591–598. https://doi.org/https://doi.org/10.1016/j.actamat.2020.02.017.

[14] M. Erol, U. Böyük, T. Volkmann, D.. Herlach, Containerless solidification of Ag–Al and Ag–Cu eutectic alloys in a drop tube, J. Alloys Compd. 575 (2013) 96–103.

LIST OF FIGURES